Article

Journal of the Brazilian Chemical Society

https://dx.doi.org/10.21577/0103-5053.20240043

J. Braz. Chem. Soc. **2024**, *35*, 10, e-20240043, 1-11

Interactive Profile between 1,4-Naphthoquinone Derivatives and Human Serum Albumin

Romulo C. Ferreira,[a,b] Otávio Augusto Chaves,[,c,d] Cosme Henrique C. S. de Oliveira,[a] Vitor Francisco Ferreira,[e] Sabrina B. Ferreira,[f] Carlos Serpa,[c] Dari Cesarin-Sobrinho[a] and José Carlos Netto-Ferreira[*,a]*

[a]*Departamento de Química Orgânica, Instituto de Química, Universidade Federal Rural do Rio de Janeiro, Rodovia BR-465, Km 7, 23890-000 Seropédica-RJ, Brazil*

[b]*Instituto Federal de Ciência e Tecnologia de Mato Grosso, Campus Juína Linha J s/n, Zona Rural, 78320-000 Juína-MT, Brazil*

[c]*CQC-IMS, Departamento de Química, Universidade de Coimbra, Rua Larga s/n, 3004-535 Coimbra, Portugal*

[d]*Laboratório de Imunofarmacologia, Centro de Pesquisa, Inovação e Vigilância em COVID-19 e Emergências Sanitárias, Instituto Oswaldo Cruz, Fundação Oswaldo Cruz, 21040-361 Rio de Janeiro-RJ, Brazil*

[e]*Departamento de Química Orgânica, Instituto de Química, Universidade Federal Fluminense, 24020-150 Niterói-RJ, Brazil*

[f]*Departamento de Química Orgânica, Instituto de Química, Universidade Federal do Rio de Janeiro, Ilha do Fundão, 21941-909 Rio de Janeiro-RJ, Brazil*

The interactive profile between four 1,4-naphthoquinone derivatives (**1-4**) and human serum albumin (HSA) was studied by spectroscopic techniques and *in silico* calculations. The bimolecular quenching rate constant (k_q ca. 10^{12} L mol^{-1} s^{-1}) and the time-resolved fluorescence decays indicated a static fluorescence quenching mechanism. Thus, there is a spontaneous ground-state association, and based on both Stern-Volmer, modified Stern-Volmer, and van't Hoff approaches, the association is moderate mainly driven by hydrophobic forces. The circular dichroism (CD) analysis indicated that until the proportion albumin:compound of 1:8 there is a weak perturbation on the structural content of albumin, while molecular docking results suggested subdomain IIA (site I), a positive electrostatic pocket, as the main binding site. Overall, even though the hydrogen atom replacement by methyl, fluorine, or chlorine atoms in the *para* position of the aromatic ring in the benzo[*g*]chromene-5,10-dione moiety changes the lipophilicity, it does not change the binding profile to HSA.

Keywords: serum albumin, 1,4-naphthoquinones, *in silico* calculations, spectroscopy

Introduction

Naphthoquinones are substances found in large amounts in higher plants, fungi, and echinoderms.[1] Lapachol and other quinones are important representatives of the contribution of popular medicine to treating human diseases in Latin America. Naphthoquinones are chemical constituents of various species of *Tabebuia*,[2-4] for example, the 2,2-dimethyl-3,4-dihydro-5,10-dioxo-2*H*-benzo[*g*]chromanone (α-lapachone) can be extracted from Brazilian medicinal plants, such as *Tabebuia* (Bignoniaceae).[5-7] It has been evaluated in terms of potential antimicrobial against multidrug-resistant bacteria.[8] This naphthoquinone and its derivatives show several biological activities, such as microbicidal properties, trypanocide, virucidal, antitumor, inhibitors of repairing cellular systems,

*e-mail: otavioaugustochaves@gmail.com; jcnetto.ufrrj@gmail.com

Editor handled this article: Carlos Maurício R. de Sant'Anna (guest)

This work is dedicated to the honorable Prof Eliezer J. Barreiro for his notable contributions to Brazilian Medicinal Chemistry.

and deoxyribonucleic acid (DNA) cleavage.[7,9-11] These quinones induce the formation of reactive oxygen species being attributed as their main biological mechanism.[12-16] Thus, α-lapachone, its derivatives, and analogs are strong candidates for developing new drugs.

Human serum albumin (HSA, molecular weight 66.5 kDa) is a predominant globular protein, widely studied in the determination of pharmacokinetic profile of potential drugs.[17,18] Synthesized in the liver, the HSA concentration in plasma is around 40 mg mL^{-1},[19,20] corresponding to about 50% of the total plasma protein. HSA is the most important carrier and distributor of different compounds, e.g., amino acids, fatty acids, drugs, steroids, cations, anions, and metals (such as calcium, copper, zinc, nickel, mercury, silver, and gold).[21] Therefore, the interaction between compounds and albumin can increase the solubility of bioactive compounds in the human blood and decrease their toxicity.[17,19-33] Crystallographic analysis of the HSA structure reveals that its main binding sites for bioactive compounds are in subdomains IIA, IIIA, and IB, which are known as Sudlow's sites I, Sudlow's site II, and site III, respectively.[17,25-27,31-33] Sites I, II, and III are known as the warfarin, benzodiazepine, and porphyrin binding regions, respectively.[34] A comparison between these three sites indicates that site I corresponds to a large hydrophobic cavity containing the tryptophan residue (Trp-214) and can be considered the more versatile site due to its capacity for binding with different compounds.[35,36]

Recently, our group reported the interactive profile of α-lapachone (1,4-naphthoquinone) with albumin.[37] To get further information on the interaction between HSA and other 1,4-naphthoquinones showing biological activity,[38] it was performed biophysical analysis (UV-Vis absorption, steady-state fluorescence, circular dichroism, time-resolved fluorescence, and molecular docking) on the interaction between HSA with 2-phenyl-3,4-dihydro-2*H*-benzo[*g*]chromene-5,10-dione (**1**), 2-(4-chlorophenyl)-3,4-dihydro-2*H*-benzo[*g*]chromene-5,10-dione (**2**), 2-(4-fluorophenyl)-3,4-dihydro-2*H*-benzo[*g*]chromene-5,10-dione (**3**), and 2-(4-methylphenyl)-3,4-dihydro-2*H*-benzo[*g*]chromene-5,10-dione (**4**) (Figure 1). These compounds were chosen due to their reported similar minimum inhibitory concentration (MIC) values in μg mL^{-1} for *Mycobacterium tuberculosis*, presenting differences in the lipophilicity (3.42-4.03 range)[38] that might impact their residence in the bloodstream.

Experimental

Materials

The HSA and phosphate buffer solution (PBS) were purchased from Merck KGaA company (Darmstadt, Germany). The 1,4-naphthoquinones derivatives **1-4** were synthesized following a literature procedure.[38] The one-pot reaction involves an initial Knoevenagel condensation of lawsone with formaldehyde, followed by a reaction with styrene or the substituted styrene in an ethanol/water mixture, yielding the corresponding 1,4- naphthoquinones. All compounds were purified by silica gel column chromatography, and spectroscopic and spectrometric data fully agree with the proposed structures.[38,39]

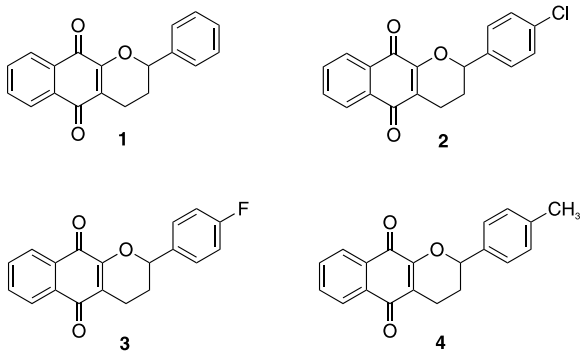

Figure 1. 2D-structure for the 1,4-naphthoquinones **1**-**4**.

Stock solutions of the 1,4-naphthoquinone derivatives (10^{-3} mol L^{-1}) were prepared in spectrophotometric grade methanol purchased from Vetec Química Fina, Brazil. Milli-Q water was obtained from Direct System QUV3-Millipore, 297 K and 18.2 mΩ.

UV-Vis and steady-state fluorescence analysis

The UV-Vis absorption and steady-state fluorescence spectra were measured in a single mode in a coupled spectrophotometer Jasco, model J-8159 (Jasco Easton, MD, USA). The apparatus had a thermostat system Jasco PFD-425S15F and a 1.0 cm quartz cell was used. All spectra were recorded with appropriate background corrections. The UV-Vis absorption spectra of the 1,4-naphthoquinone derivatives (1×10^{-3} mol L^{-1}, in PBS) were obtained from 200 to 450 nm. The UV spectra for 3 mL of HSA solution (1×10^{-5} mol L^{-1}) were recorded without and after successive increase of naphthoquinones concentration (0; 0.340; 0.670; 1.01; 1.35; 1.69; 2.02; 2.36; and 2.70×10^{-5} mol L^{-1} for **1**, 0; 0.571; 1.14; 1.70; 2.26; 2.82; 3.37; 3.92; and 4.47×10^{-5} mol L^{-1} for **2**, 0; 2.48; 4.94; 7.39; 9.82; 12.2; 14.6; 17.0; 19.4×10^{-5} mol L^{-1} for **3**, and 0; 0.678; 1.35; 2.02; 2.68; 3.34; 4.00; 4.65; and 5.30×10^{-5} mol L^{-1} for **4**) in the range of 200-330 nm at 310 K.

Steady-state fluorescence spectra were measured in the range of 300-450 nm with excitation at 280 nm at three temperatures (305, 310, and 315 K). First, the fluorescence emission spectrum of a solution containing 3 mL of HSA (1×10^{-5} mol L-1 in PBS) was obtained. In sequence, the

fluorescence quenching experiments were performed by adding the 1,4-naphthoquinone derivatives **1-4** from a stock solution in methanol (1×10^{-3} mol L^{-1}) to the HSA solution following the same concentrations used in the UV analysis. The results were analyzed using the following mathematical approaches after inner filter corrections: Stern-Volmer, modified Stern-Volmer, van't Hoff, and Gibbs' free energy.[40] The spectra used to estimate quantitatively the binding capacity of the interaction albumin:naphthoquinones were obtained by the average of three successive scans after the corresponding background corrections to posterior statistical analysis based on the linear regression. Plots were obtained by monitoring the HSA fluorescence emission at its maximum (345 nm).

Circular dichroism (CD) analysis

In the range of 200-250 nm, CD spectra were recorded at 310 K in a single mode in a coupled spectrophotometer Jasco, model J-8159 (Jasco Easton, MD, USA). The CD spectra for albumin:**1-4** were obtained in the proportion 1:0, 1:4, 1:8, 1:16, and 1:32. The CD results were expressed in terms of significant molar residual ellipticity (MRE),[41] and the decrease in the helical structure after naphthoquinones binding was quantitatively determined following literature procedure at 208 and 222 nm.[42]

Time-resolved fluorescence analysis

Spectrofluorometer model FL920 CD (Edinburgh Instruments Ltd, Livingston, UK) was used to obtain the time-resolved fluorescence decays (λ_{exc} = 280 ± 10 nm). The corresponding decays were obtained for HSA solution (1×10^{-5} mol L^{-1}) without and with each naphthoquinone at 298 K. For the naphthoquinone **1** was used the same range of concentrations used in the UV and steady-state fluorescence measurements, while for naphthoquinones **2**-**4** was used only the highest concentration.

In silico calculations

The HSA structure without any compounds is from Protein Data Bank[43] (3JRY).[44] Spartan'14 software[45-47] was used to build and energy-minimized (semi-empirical method PM6) the **1-4** structure, while GOLD 2022.3.0 software[48-50] was used to molecular docking calculations. A radius of 8 Å around Trp-214, Tyr-411, and Tyr-161 residues was established for sites I, II, and III, respectively.[25] 'ChemPLP' was used as the scoring function. For each system albumin:naphthoquinone it was obtained ten running poses and was chosen the pose with the highest docking score value for the interactive treatment. The webserver Protein-Ligand Interaction Profiler (PLIP)[51-53] was used for3 the treatment of the best docking pose, while the 3D figures were generated by PyMOL Molecular Graphics System 1.0 level software.[54,55]

Results and Discussion

Binding affinity-spectroscopic approaches

The HSA has an absorption band at a wavelength of around 280 nm, mainly attributed to the absorption of tryptophan (Trp), with a smaller contribution from tyrosine (Tyr) and phenylalanine (Phe).[25] These amino acid residues are relatively non-polar and can participate in hydrophobic interactions, which are relatively strong when aromatic groups (aromatic groups linked to the base structure of the amino acid) are positioned side by side.[56,57] The hydroxyl group of Tyr and indole group of Trp can form hydrogen bonds, acting as important functional groups when discussing enzymatic activity.[58]

The structural changes of HSA, as a function of adding the naphthoquinones, were initially studied through absorption spectra in the UV region as shown in Figure 2a. In this case, the absorption spectrum for HSA (1×10^{-5} mol L^{-1}, in PBS) in the range of 200-330 nm was recorded in the absence and presence of varying concentrations of **1**. It is not possible to conclude the formation of HSA-naphthoquinone complex by analyzing the UV absorption spectra shown in Figure 2a, as naphthoquinone **1** in PBS (inset in Figure 2a) presents absorption maxima around 250 and 285 nm, coinciding with the maximum absorption of the aromatic amino acid residues of albumin at 280 nm.[59] Thus, the explanation for both the bathochromic shift and the hyperchromic effect after the addition of **1** may result from the presence of this naphthoquinone in solution, as well as is not reliable the determination of binding constant values from UV spectra, being the steady-state fluorescence analysis (the naphthoquinones **1-4** do not show any fluorescence emission) crucial to determine the binding affinity HSA:**1-4**. Similar results were obtained for the naphthoquinones **2-4** (Figure S1 in the Supplementary Information (SI) section).

The fluorescence emission for HSA at 345 nm (λ_{exc} = 280 nm) is due to the contribution of the aromatic amino acid residues, e.g., Trp-214,[21] while in this experimental condition, the 1,4-naphthoquinone derivatives **1-4** do not show any fluorescence emission. As an example, Figure 2b depicts the fluorescence emission of albumin and the corresponding quenching in the presence of **1**, indicating that the 1,4-naphthoquinone derivative under study might

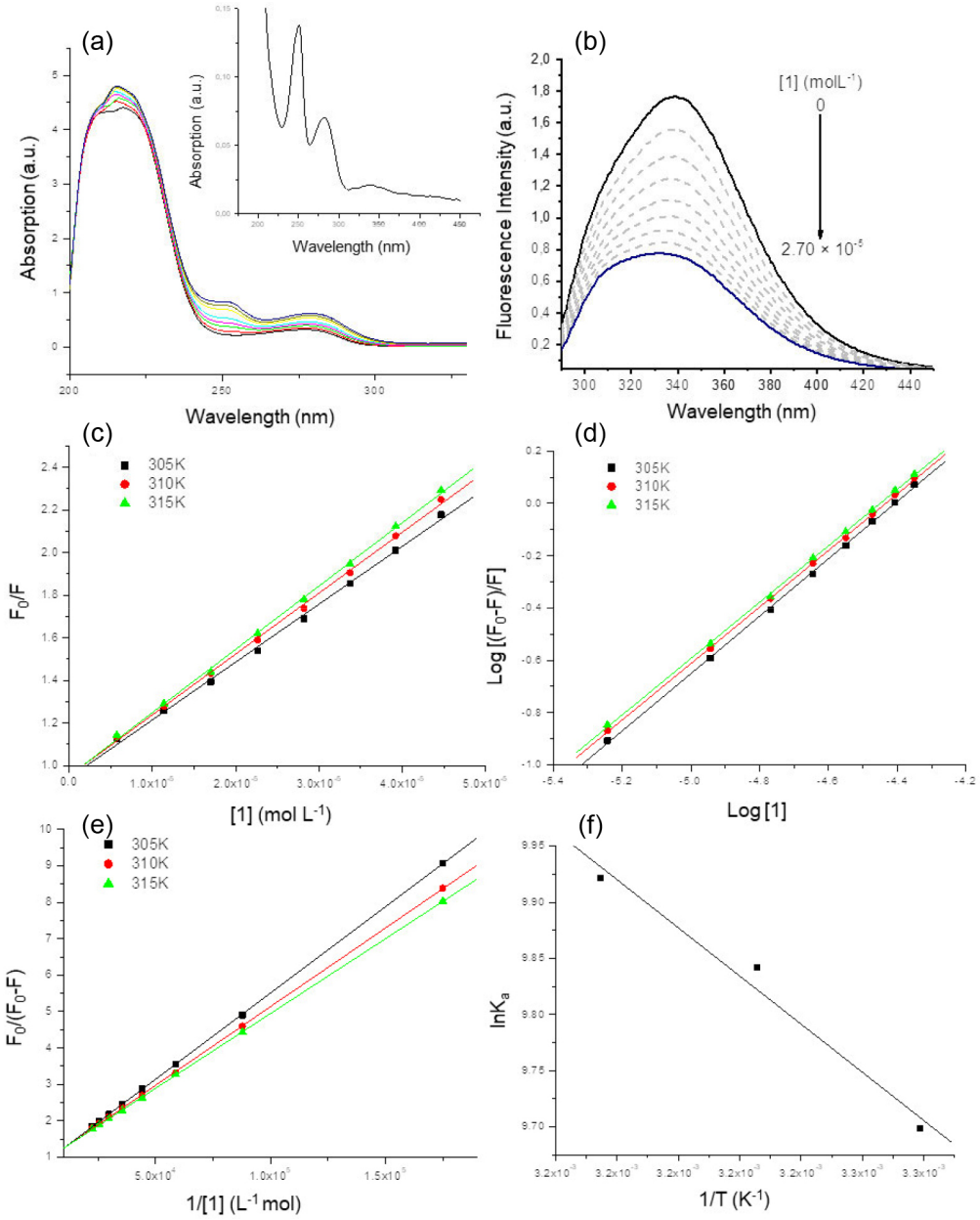

Figure 2. (a) The UV-Vis spectra for HSA solution in PBS (pH = 7.4) at 310 K, without and in the presence of **1**. (b) Steady-state fluorescence spectra for HSA and HSA:**1** at 310 K (λ_{exc} = 280 nm). (c) Stern-Volmer plots obtained at 305, 310, and 315 K. (d) Double logarithmic plots for three temperatures. (e) van't Hoff plot corresponding to the binding constant (K_a) values. $C_{(HSA)} = 1 \times 10^{-5}$ mol L^{-1}. $C_{(1)}$ = 0; 0.340; 0.670; 1.01; 1.35; 1.69; 2.02; 2.36; and 2.70×10^{-5} mol L^{-1}. Inset: absorption spectrum for **1** in PBS.

interact close to the fluorophores of albumin.[60,61] The increase of the naphthoquinone concentration leads to a slight blue shift in the maximum fluorescence emission, suggesting a decrease in the polarity of the interactive pocket after naphthoquinone binding.[19] Similar behavior was observed for the 1,4-naphthoquinones **2-4** as shown in Figures S2-S4 in the SI section.

Fluorescence quenching can involve two possible mechanisms, i.e., dynamic, or static mechanism.[60] To identify the possible fluorescence quenching mechanism operating in this case, Stern-Volmer analysis was applied, following the literature.[58,62] The Stern-Volmer plots corresponding to the fluorescence quenching of HSA by **1** at 305, 310, and 315 K, are shown in Figure 2c, while for the 1,4-naphthoquinones **2-4** are shown in Figures S2-S4 in the SI section, and the calculated Stern-Volmer (K_{SV}) and bimolecular quenching rate (k_q) constant values are summarized in Table 1. The K_{SV} and k_q values among the 1,4-naphthoquinones derivatives are in the same order of magnitude, indicating that the replacement of small groups in the aromatic moiety of the compounds does not change the affinity to the albumin.

Since the Stern-Volmer plots are linear and the k_q values are much higher than the diffusion rate constant in water (k_{diff} ca. 7.40×10^9 L mol^{-1} s^{-1} at 298 K, according to Smoluchowski-Stokes-Einstein theory),[63] the quenching mechanism resulting from the interaction between HSA and **1-4** must be static, consequence of a ground-state association HSA:naphthoquinone. These K_{SV} and k_q values were similar to those reported for other 1,4-naphthoquinones, such as 2-phenyl-2,3-dihydronaphtho[2,3-*b*]furan-4,9-dione, 2-(4-bromophenyl)-2,3-dihydronaphtho[2,3-*b*]furan-4,9-dione, and 2-(benzylamino)-1,4-naphthoquinone.[37,40]

Further confirmation that the main mechanism of fluorescence quenching is static was obtained by determining the fluorescence lifetimes in the absence and presence of naphthoquinones **1-4**. The HSA fluorescence presents three components with considerably different lifetimes. The two shortest lifetimes are associated with the Trp structure itself, and the third is related to the Trp-214 surrounding environment interaction.[64,65] The first lifetime is very short (sub nanosecond) with a low pre-exponential factor (3%). Thus, due to the instrumental limitations, most reports (as we in the present work) observed solely two lifetimes.[61] The obtained fluorescence lifetime (τ) for free HSA in PBS at room temperature has two distinct components with different contributions, i.e., τ_1 = 1.56 (33.8% contribution) and τ_2 = 5.30 ns (66.2% contribution), agreeing with the literature.[66,67] After the successive addition of aliquots of a stock solution of naphthoquinone **1** to the protein solution, up to a maximum compound concentration of 2.70×10^{-5} mol L^{-1}, no significant variation in the fluorescence lifetime for albumin was observed (Figure 3 and Table 2). For this reason, further fluorescence quenching experiments with the naphthoquinones **2-4** were performed employing only the maximum concentration of the quencher (Table 2). In all cases, time-resolved fluorescence quenching confirmed the static mechanism proposed from the experiments described above for the albumin fluorescence quenching study in the steady-state analysis.[58]

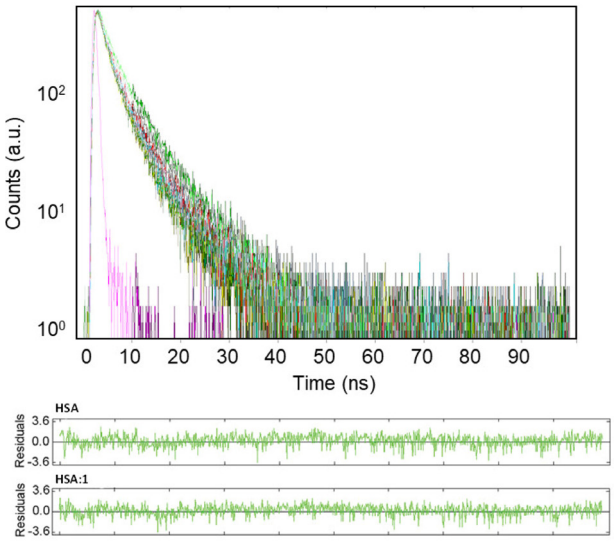

Figure 3. Time-resolved fluorescence results for HSA in the absence and with different concentrations of **1** in PBS (pH = 7.4) at 298 K. The residual corresponds to HSA and HSA:**1** without and in the maximum naphthoquinone concentration, respectively. The short decay corresponds to the instrument response function (IRF, a suspension of TiO_2 in water and glycerol). $C_{(HSA)} = 1 \times 10^{-5}$ mol L^{-1}. $C_{(1)}$ = 0; 0.340; 0.670; 1.01; 1.35; 1.69; 2.02; 2.36; and 2.70×10^{-5} mol L^{-1}.

A purely ground-state association also indicates one binding site of albumin to one compound, and this was reinforced by the number of binding site (n)

Table 1. The quantitative binding parameters for the interaction HSA:**1**-**4** in PBS

Sample	T / K	K_{SV}[a] / ($\times 10^4$ L mol^{-1})	k_q[a] / ($\times 10^{12}$ L mol^{-1} s^{-1})	n[b]	K_a[c] / ($\times 10^4$ L mol^{-1})
HSA:**1**	305	2.72 ± 0.05	5.17 ± 0.09	1.09 ± 0.05	1.63 ± 0.01
	310	2.86 ± 0.04	5.44 ± 0.08	1.08 ± 0.04	1.88 ± 0.02
	315	2.97 ± 0.04	5.65 ± 0.08	1.08 ± 0.05	2.04 ± 0.02
HSA:**2**	305	4.53 ± 0.02	8.61 ± 0.04	1.00 ± 0.06	4.68 ± 0.01
	310	4.32 ± 0.08	8.21 ± 0.10	0.95 ± 0.05	6.15 ± 0.01
	315	4.21 ± 0.05	8.00 ± 0.09	0.93 ± 0.05	7.05 ± 0.01
HSA:**3**	305	5.56 ± 0.04	10.6 ± 0.08	1.09 ± 0.04	3.61 ± 0.08
	310	5.20 ± 0.06	9.89 ± 0.11	1.06 ± 0.05	3.63 ± 0.02
	315	4.83 ± 0.04	9.18 ± 0.08	1.05 ± 0.05	3.65 ± 0.02
HSA:**4**	305	3.96 ± 0.05	7.53 ± 0.09	1.11 ± 0.04	2.45 ± 0.03
	310	3.57 ± 0.04	6.79 ± 0.08	1.10 ± 0.04	2.34 ± 0.02
	315	3.31 ± 0.05	6.29 ± 0.09	1.08 ± 0.05	2.27 ± 0.05

[a]r^2 (coefficient of determination, dimensionless) values for the Stern-Volmer constant (K_{sv}) and bimolecular quenching rate constant (k_q) in the range of 0.9975-0.9991; [b]r^2 values for the number of binding sites (n) in the range of 0.9981-0.9995, [c]r^2 values for the binding constant (K_a) in the range of 0.9987-0.9990. HSA: human serum albumin; T: temperature.

Table 2. Fluorescence lifetimes for HSA without and with 1,4-naphthoquinones **1-4**

Sample	[Naphthoquinone] / (10^{-5} mol L^{-1})	τ_1 / ns	τ_2 / ns	χ^2	τ_1 relative / %	τ_2 relative / %
	0	1.56	5.30	1.040	33.8	66.2
	0.340	1.38	5.29	1.119	28.7	71.3
	0.670	1.64	5.25	0.985	39.3	60.7
	1.01	1.54	5.20	1.030	25.5	74.5
HSA:**1**	1.35	1.39	5.17	0.950	34.9	65.1
	1.69	1.34	5.15	0.914	40.9	59.1
	2.02	1.33	5.10	0.967	41.9	58.1
	2.36	1.16	5.08	1.066	37.3	62.7
	2.70	1.23	5.05	1.065	33.9	65.1
HSA:**2**	4.47	1.49	5.14	0.921	36.3	63.7
HSA:**3**	19.4	1.70	5.26	1.052	28.7	71.3
HSA:**4**	5.30	1.35	5.04	1.095	43.0	57.0

HSA: human serum albumin; τ_1 and τ_2: the first and second lifetimes, respectively; χ^2 (chi squared): measures the goodness of fit of experimental data to a bi-exponential decay.

values close to 1 determined via double-logarithmic approach (Table 1, Figure 2d, and Figures S2-S4 in the SI section).[25] In addition, in a static mechanism, the K_{SV} values also indicate the binding affinity.[58,68] Since the K_{SV} values are around 10^4 L mol^{-1}, there is a moderate binding affinity,[69,70] following the same behavior of α-lapachone and other reported 1,4-naphthoquinones.[37,40] Additionally, in this case, the fluorescence data was obtained not exciting exclusively the Trp-214 residue, but also the Tyr and Phe residues (λ_{exc} 280 nm), thus, another mathematical treatment, namely modified Stern-Volmer approximation, was applied to also estimate the binding capacity (Figure 2e).[58] The binding constant (K_a) values are in the same order of magnitude compared to K_{SV} (Table 1), reinforcing the moderate binding affinity of the 1,4-naphthoquinones to albumin.[68-70]

From the K_a values calculated by HSA fluorescence quenching experiments, van't Hoff plots were constructed to determine the thermodynamic parameters (enthalpy and entropy change, ΔH° and ΔS°, respectively)[58] (Figure 2f for HSA:**1** and Figure S5 in the SI section for HSA:**2-4**). All thermodynamic values are summarized in Table 3. The negative values for the Gibbs' free energy change (ΔG°) indicate that all the 1,4-naphthoquinones bind spontaneously with the albumin, being entropically driven, however, for the naphthoquinone **4**, the ΔH° value also corroborated with the spontaneity of the binding, being also considered enthalpically driven. Additionally, following Ross and Subramanian approaches[71] $\Delta S^o > 0$ and $\Delta H^o > 0$ often lead to evidence that the predominance interaction is hydrophobic, while $\Delta H^o < 0$ could indicate the occurrence of a hydrophilic interaction with the possible formation of hydrogen bonds. The obtained thermodynamic parameters follow the same trend previously reported to 2-(benzylamino)-1,4-naphthoquinone, 2-[(2'-hydroxypropyl)amino]-1,4-naphthoquinone, and 2-[(2'-hydroxyethyl)amino]-1,4-naphthoquinone.[40]

Table 3. Thermodynamic parameters obtained from van't Hoff plots for the fluorescence quenching of HSA by naphthoquinones **1-4**

Sample	T / K	ΔH^0 / (kJ mol^{-1})	ΔS^0 / (J mol^{-1} K^{-1})	ΔG^0 / (kJ mol^{-1})
	305			–24.9
HSA:**1**	310	17.8	140	–25.6
	315			–26.3
	305			–27.5
HSA:**2**	310	32.9	198	–28.5
	315			–29.5
	305			–20.7
HSA:**3**	310	0.920	71.0	–21.1
	315			–21.4
	305			–25.0
HSA:**4**	310	–6.12	62.0	–25.3
	315			–25.7

HSA: human serum albumin; T: temperature; ΔH°: enthalpy change; ΔS°: entropy change; ΔG°: Gibbs' free energy change; r^2: coefficient of determination (dimensionless) in the range of 0.9940-0.9981.

Estimation of the secondary structure of HSA

The CD spectra were obtained to evaluate the structural content of HSA without and with 1,4-naphthoquinones **1-4**. The CD spectra obtained for HSA without and with different proportions of **1** at 310 K are shown in Figure 4, while for the remaining naphthoquinones, i.e., **2-4**, are shown in Figure S6 in the SI section. The CD spectra for HSA in the presence of **1-4** exhibit two negative signals (negative Cotton effects) with minimum peaks in the UV

region. These absorptions correspond to π-π* (208 nm) and n-π* (222 nm) transitions, characteristics of the helical content.[25] The CD spectra for free HSA and in the presence of naphthoquinones **1-4** have similar profiles, with an increase in the intensities of both bands at 208 and 222 nm in the presence of the naphthoquinones, indicating that the HSA structure consists predominantly of α-helix content even after bound with **1-4**, reinforcing the moderate interactive profile previously identified by the steady-state fluorescence analysis.[72]

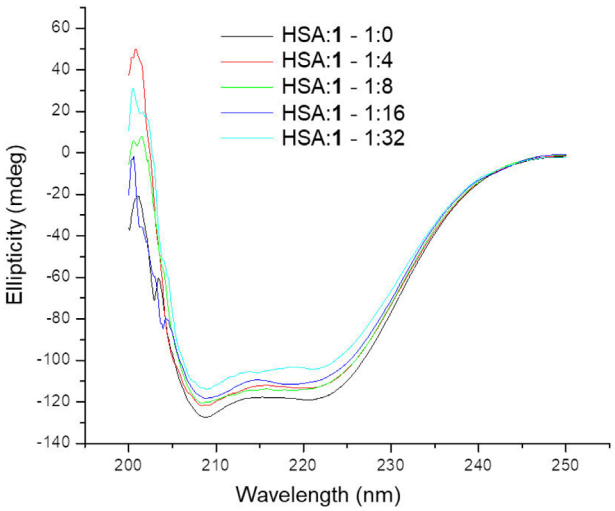

Figure 4. The CD spectra for HSA without and with different proportions of 1,4-naphthoquinone **1** (1:0, 1:4, 1:8, 1:16, and 1:32) at 310 K. $C_{(HSA)} = 1 \times 10^{-6}$ mol L^{-1}.

The percentage of α-helix content for free HSA and HSA bound with **1-4** in different proportions of 1,4-naphthoquinones was summarized in Table 4. The quantitative results indicate that until the proportion HSA:naphthoquinone of 1:8 the binding perturbs weakly the secondary structure of albumin, however, in the proportions 1:16 and 1:32 the perturbation is more significative, following the same trend reported to α-lapachone.[37]

In silico calculations

The HSA structure has three main feasible binding sites: subdomain IIA (site I), where Trp-214 residues can be found, subdomain IIIA (site II), and subdomain IB (site III).[27,73-75] Thus, to suggest the main binding pocket of HSA to the 1,4-naphthoquinones under study, as well as identify the main intermolecular forces responsible for the stabilization of the complex, *in silico* calculations via molecular docking were carried out.[76,77] Table 5 summarizes the docking score values for HSA:**1-4** in the three feasible binding sites. The highest docking score value (dimensionless) was obtained for site I, thus, *in silico* calculations suggested subdomain IIA as the main binding site, however, the docking score value between subdomains IIA and IB are quite similar, indicating the 1,4-naphthoquinones might interact not exclusively with site I, probably due to the low steric volume of the compounds making them favorable to interact in different

Table 4. The α-helix at 208 and 222 nm for HSA (pH = 7.4) at 305, 310, and 315 K without and with different concentrations of naphthoquinones **1-4**

Sample		α-Helix / %					
	T / K	305		310		315	
	θ / mdeg	208	222	208	222	208	222
HSA:**1**	1:0	60.9	59.2	59.2	58.5	60.0	57.1
	1:4	57.9	56.1	55.5	54.9	58.0	55.0
	1:8	57.2	56.0	54.9	53.1	57.5	54.2
	1:16	51.0	58.4	51.5	49.6	55.4	52.3
	1:32	47.6	51.0	51.4	47.9	54.2	50.4
HSA:**2**	1:0	60.8	58.5	58.8	55.7	58.4	56.4
	1:4	57.6	56.6	55.2	53.4	58.2	55.1
	1:8	57.0	54.8	54.0	51.3	55.4	51.9
	1:16	53.7	51.0	49.4	46.3	53.8	51.6
	1:32	46.5	45.7	46.1	43.1	48.4	46.5
HSA:**3**	1:0	60.2	58.2	57.9	55.3	60.7	58.2
	1:4	58.7	56.7	56.3	54.3	60.1	56.9
	1:8	58.4	54.8	55.2	54.1	56.2	54.5
	1:16	55.7	52.8	53.2	53.1	54.1	50.6
	1:32	51.3	49.3	48.2	49.1	52.4	49.3
HSA:**4**	1:0	59.7	57.7	58.2	56.1	60.8	58.3
	1:4	58.3	56.4	57.8	54.5	58.9	55.9
	1:8	56.7	55.6	55.2	53.7	56.0	55.4
	1:16	54.7	54.8	54.0	52.7	57.0	54.3
	1:32	53.7	53.3	50.9	50.0	51.8	51.7

HSA: human serum albumin; T: temperature; θ: the observed circular dichroism signal (in milli-degrees).

Table 5. Docking score values (dimensionless) for HSA:**1-4**

Sample	Site I	Site II	Site III
HSA:**1**	64.3	48.1	61.4
HSA:**2**	59.8	54.0	57.8
HSA:**3**	65.9	53.8	61.5
HSA:**4**	60.8	53.9	57.4

HSA: human serum albumin.

binding pockets. Comparing the experimental steady-state fluorescence data with the *in silico* results, both indicated that there is not any significant difference in the binding affinity among **1-4** and albumin.

Figure 5 depicts the superposition of the best docking pose with the corresponding interactive profile. Molecular docking results suggested a superposition among the 1,4-naphthoquinones **1-4** mainly into subdomain IIA than into subdomain IB (Figures 5a and 5b), reinforcing the hypothesis that the main binding site might be site I (similar binding affinity approach). Additionally, the compounds are more buried into the positive electrostatic potential

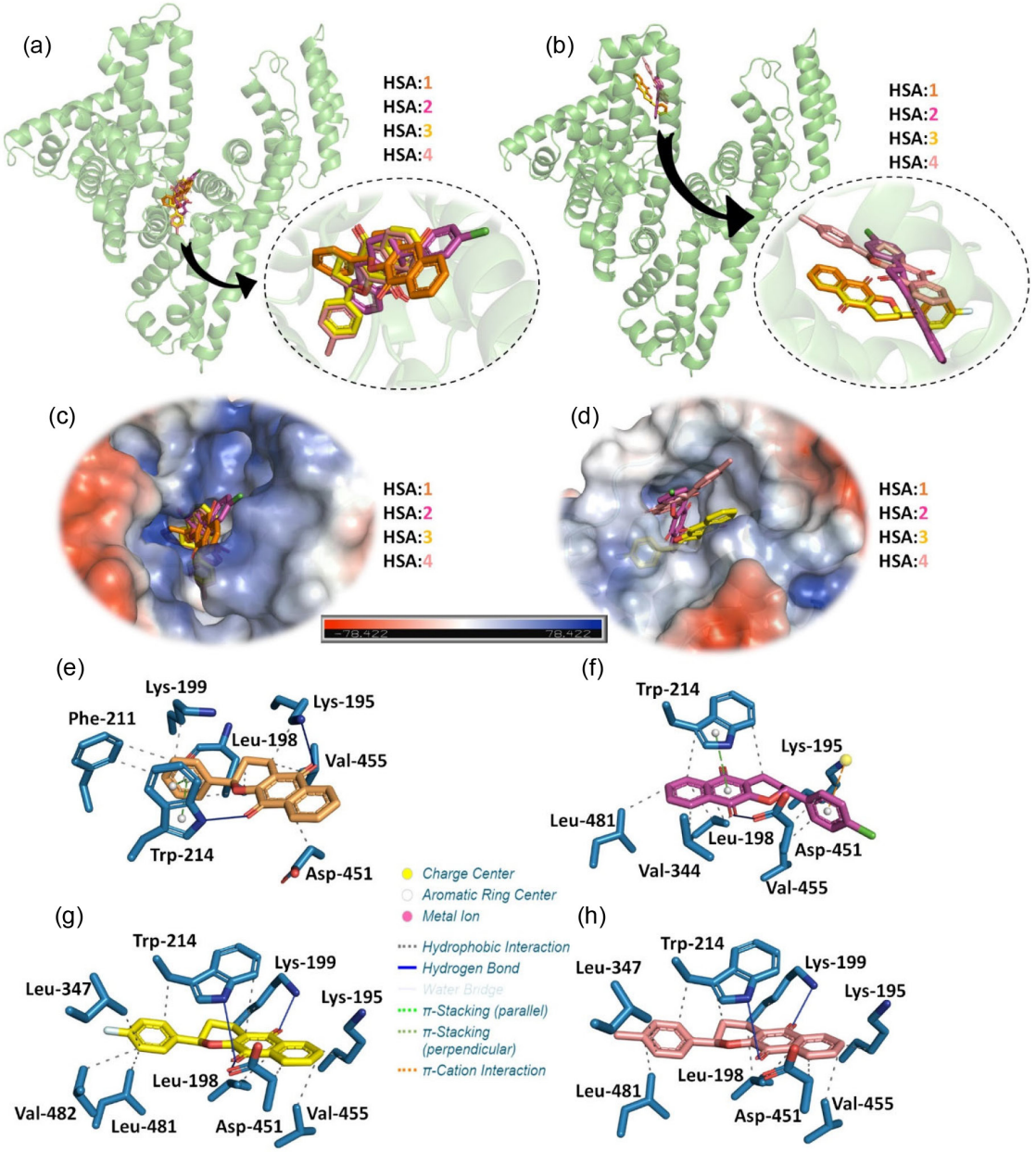

Figure 5. Superposition of the docking pose with the corresponding zoom representation for HSA:**1-4** in the (a) site I and (b) site II. The electrostatic potential map of albumin in the presence of **1-4** in the (c) site I and (d) site II. Representation of the amino acid residues and the corresponding interactive forces with the 1,4-naphthoquinones (e) **1**, (f) **2**, (g) **3**, and (h) **4** into subdomain IIA. Selected amino acid residues, **1**, **2**, **3**, and **4** are in blue, orange, pink, yellow, and beige, respectively. Color of the elements: nitrogen, oxygen, chloro, and fluorine in dark blue, red, green, and cyan, respectively. The hydrogen atoms were omitted for better interpretation.

pocket of site I than site II (Figures 5c and 5d), interacting with the main fluorophore of albumin (Trp-214 residue, Figures 5e-5h), agreeing with the experimental ground-state association. Finally, molecular docking calculations suggested hydrophobic interaction as the key forces to stabilize the complex formation, corroborating with the experimental thermodynamic analysis, however, in some cases, the *in silico* results also identified some contribution of hydrophilic interactions, such as hydrogen bond and π-cation forces.

Conclusions

The 1,4-naphthoquinones **1-4** interacted spontaneously with HSA via a ground-state association driven by entropy effects, however, for HSA:**4** there is a contribution from enthalpy. The obtained K_{SV} and K_a values are in the same order of magnitude (10^4 L mol^{-1}), indicating a moderate binding capacity with similar binding affinity compared with other 1,4-naphthoquinones, e.g., α-lapachone, 2-(benzylamino)-1,4-naphthoquinone, 2-[(2'-hydroxypropyl)amino]-1,4-naphthoquinone, and 2-[(2'-hydroxyethyl)amino]-1,4-naphthoquinone. The binding perturbs weakly the secondary structure of albumin until the proportion albumin:compound of 1:8, and the 1,4-naphthoquinones can interact not only with subdomain IIA, where Trp-214 residue can be found but also with subdomain IB (both in a positive electrostatic potential region), mainly via hydrophobic forces, corroborating with the thermodynamic trend. Overall, even though the hydrogen atom replacement by methyl, fluorine, or chlorine atoms in the *para* position of the aromatic ring in the benzo[*g*]chromene-5,10-dione moiety changes the lipophilicity, it does not change the binding profile to HSA.

Supplementary Information

Supplementary information (spectroscopic analysis on the interactive profile between HSA and 2-4) is available free of charge at http://jbcs.sbq.org.br. as PDF file.

Acknowledgments

The authors acknowledge the Brazilian financing agencies: Coordenação de Aperfeiçoamento de Pessoal de Nível Superior (CAPES), Conselho Nacional do Desenvolvimento Científico e Tecnológico (CNPq), and Fundação de Amparo à Pesquisa do Estado do Rio de Janeiro (FAPERJ) for the fellowships and research grants. Additionally, the authors also acknowledge the Coimbra Chemistry Centre which is supported by the Fundação para a Ciência e a Tecnologia (FCT- Portuguese Agency for Scientific Research) through the projects UIDB/00313/2020 and UIDP/00313/2020. O. A. C. thanks FCT for his PhD fellowship 2020.07504.BD.

Author Contributions

R. C. Ferreira was responsible for formal analysis, data curation, visualization, methodology, investigation, writing original draft; O. A. Chaves for formal analysis, data curation, visualization, methodology, validation, software, investigation, project administration, supervision, writing (original draft, review and editing); C. H. C. S. Oliveira for formal analysis, investigation; V. F. Ferreira for visualization; S. B. Ferreira for visualization; C. Serpa for visualization, formal analysis, writing (review and editing); D. Cesarin-Sobrinho for formal analysis, visualization, investigation; J. C. Netto-Ferreira for conceptualization, funding acquisition, visualization, validation, methodology, investigation, project administration, supervision, writing (original draft, review and editing).

References

1. Lemos, T. G.; Monte, F. J. Q.; Santos, A.K. L.; Fonseca, A. M.; Santos, H. S.; Oliveira, M. F.; Costa, S. M. O.; Pessoa, O. D. L.; Braz-Filho, R.; *Nat. Prod. Res.* **2007**, *21*, 529. [Crossref]
2. Hamed, A. N. E.; Mahmoud, B. K.; Samy, M. N.; Kamel, M. S.; *J. Herbal Med*. **2020**, *24*, 100410. [Crossref]
3. Viegas Jr., C.; Bolzani, V. S.; Barreiro, E. J.; *Quim. Nova* **2006**, *29*, 326. [Crossref]
4. Pinto, A. C.; Silva, D. H. S.; Bolzani, V. S.; Lopes, N. P.; Epifanio, R. A.; *Quim. Nova* **2002**, *25*, 45. [Crossref]
5. de Moura, K. C. G.; Emery, F. S.; Neves-Pinto, C. L.; Pinto, M. C. F. R.; Dantas, A. P.; Salomão, K.; de Castro, S. L.; Pinto, A. V.; *J. Braz. Chem. Soc.* **2001**, *12*, 325. [Crossref]
6. Fujii, N.; Yamashita, Y.; Mizukami, T.; Nakano, H.; *Mol. Pharmacol*. **1997**, *51*, 269. [Crossref]
7. Krishnam, P.; Bastow, K. F.; *Biochem. Pharmacol.* **2000**, *60*, 1367. [Crossref]
8. Machado, T. B.; Pinto, A. V.; Pinto, M. C. F. R.; Leal, I. C. R.; Silva, M. G.; Amaral, A. C. F.; Kuster, R. M. A.; Santos, K. R. N.; *Int. J. Antimicrob. Agents* **2003**, *84*, 279. [Crossref]
9. Li, C. J.; Averboukh, L.; Pardee, A. B.; *J. Biol. Chem.* **1993**, *30*, 22463. [Crossref]
10. Krishnan, P.; Bastow, K. F.; *Cancer Chemother. Pharmacol*. **2001**, *47*, 187. [Crossref]
11. Huang, L.; Pardee, A. B.; *Mol. Med.* **1999**, *5*, 711. [Crossref]
12. Docampo, R.; Cruz, F. S.; Boveris, A.; Muniz, R. P. A.; Esquivel, D. M. S.; *Biochem. Pharmacol.* **1979**, *28*, 723. [Crossref]
13. Powis, G.; *Pharmacol. Ther.* **1987**, *35*, 57. [Crossref]
14. Santos, D. M.; Santos, M. M. M.; Moreira, R.; Solá, S.; Rodrigues, C. M. P.; *Mol. Neurobiol*. **2013**, *47*, 313. [Crossref]

15. Baptista, M. S.; Cadet, J.; Di Mascio, P.; Ghogare, A. A.; Greer, A.; Hamblin, M. R.; Lorente, C.; Nunez, S. C.; Ribeiro, M. S.; Thomas, A. H.; Vignoni M.; Yoshimura, T. M.; *Photochem. Photobiol.* **2017**, *93*, 912. [Crossref]
16. Bombaça, A. C. S.; Silva, L. A.; Chaves, O. A.; da Silva, L. S.; Barbosa, J. M. C.; da Silva, A. M.; Ferreira, A. B. B.; Menna-Barreto, R. F. S.; *Biomed. Pharmacother.* **2021**, *135*, 111186. [Crossref]
17. Zsila, F.; Bikádi, Z.; Simonyi, M.; *Biochem. Pharmacol.* **2003**, *65*, 447. [Crossref]
18. Takehara, K.; Yuri, K.; Shirasawa, M.; Yamasaki, S.; Yamada, S.; *Anal. Sci.* **2009**, *25*, 115. [Crossref]
19. Tang, J.; Qi, S.; Chen, X.; *J. Mol. Struct.* **2005**, *779*, 87. [Crossref]
20. Chaves, O. A.; Amorim, A. P. O.; Castro, L. H. E.; Sant'Anna, C. M. R.; de Oliveira, M. C. C.; Cesarin-Sobrinho, D.; Netto-Ferreira, J. C.; Ferreira, A. B. B.; *Molecules* **2015**, *20*, 19526. [Crossref]
21. Rabbani, G.; Ahn, S. N.; *Int. J. Biol. Macromol.* **2021**, *193*, 948. [Crossref]
22. Sugio, S.; Kashima, A.; Mochizuki, S.; Noda, M.; Kobayashi, K.; *Protein Eng*. **1999**, *12*, 439. [Crossref]
23. He, X. M.; Carter, D. C.; *Nature* **1992**, *358*, 209. [Crossref]
24. Bhattacharya, A. A.; Curry, S.; Franks, N. P.; *J. Biol. Chem.* **2000**, *275*, 38731. [Crossref]
25. Chaves, O. A.; Loureiro, R. J. S.; Costa-Tuna, A.; Almeida, Z. L.; Pina, J.; Brito, R. M. M.; Serpa, C.; *ACS Food Sci. Technol.* **2023**, *3*, 955. [Crossref]
26. Tang, J.; Luan, F.; Chen, X.; *Bioorg. Med. Chem.* **2006**, *14*, 3210. [Crossref]
27. Park, J.; Kim, M.-S.; Park, T.; Kim, Y. H.; Shin, D. H.; *Int. J. Biol. Macromol.* **2021**, *166*, 221. [Crossref]
28. Noh, E.; Moon, J. M.; Chun, B. J.; Cho, Y. S.; Ryu, S.; Kim, D.; *Basic Clin. Pharmacol. Toxicol.* **2021**, *128*, 605. [Crossref]
29. Belinskaia, D. A.; Voronina, P. A.; Shmurak, V. I.; Jenkins, R. O.; Goncharov, N. V.; *Int. J. Mol. Sci.* **2021**, *22*, 10318. [Crossref]
30. Li, J.; Ren, C.; Zhang, Y.; Liu, X.; Yao, X.; Hu, Z.; *J. Mol. Struct.* **2008**, *885*, 64. [Crossref]
31. Shaw, A. K.; Pal, S. K.; *J. Photochem. Photobiol., B* **2008**, *90*, 69. [Crossref]
32. Li, S.; Wang, L.; Hao, J.; Wang, L.; Tong, Y.-J.; Fu, Z.-Q.; Zhang, A.-P.; *J. App. Spectrosc.* **2017**, *83*, 1076. [Crossref]
33. Zhang, J.; Xiong, D.; Chen, L.; Kang, Q.; Zeng, B.; *Spectrochim. Acta, Part A* **2012**, *96*, 132. [Crossref]
34. Rabbani, G.; Ahn, S. N.; *Int. J. Biol. Macromol.* **2019**, *123*, 979. [Crossref]
35. Petitpas, I.; Bhattacharya, A. A.; Twine, S.; East, M.; Curry, S.; *J. Biol. Chem.* **2001**, *276*, 22804. [Crossref]
36. Stan, D.; Matei, I.; Mihailescu, C.; Savin, M.; Matache, M.; Hillebrand, M.; Baciu, I.; *Molecules* **2009**, *14*, 1614. [Crossref]
37. Chaves, O. A.; Schaeffer, E.; Sant'Anna, C. M. R.; Netto-Ferreira, J. C.; Cesarin-Sobrinho, D.; Ferreira, A. B. B.; *Mediterr. J. Chem.* **2016**, *5*, 331. [Crossref]
38. Ferreira, S. B.; da Silva, F. C.; Bezerra, F. A. F. M.; Lourenço, M. C. S.; Kaiser, C. R.; Pinto, A. C.; Ferreira, V. F.; *Arch. Pharm. Chem. Life Sci.* **2010**, *343*, 81. [Crossref]
39. Freire, C. P. V.; Ferreira, S. B.; de Oliveira, N. S. M.; Matsuura, A. B. J.; Gama, I. L.; da Silva, F. D. C.; de Souza, M. C. B. V.; Lima E. S.; Ferreira, V. F.; *MedChemComm* **2010**, *1*, 229. [Crossref]
40. da Silva, C. C.; Chaves, O. A.; Paiva, R. O.; da Costa, G. L.; Netto-Ferreira, J. C.; Echevarria, A.; *J. Braz. Chem. Soc.* **2020**, *31*, 1838. [Crossref]
41. Chaves, O. A.; Santos, M. R. L.; Oliveira, M. C. C.; Sant'Anna, C. M. R.; Ferreira, R. C.; Echevarria, A.; Netto-Ferreira, J. C.; *J. Mol. Liq.* **2018**, *254*, 280. [Crossref]
42. Chaves, O. A.; de Barros, L. S.; Oliveira, M. C. C.; Sant'Anna, C. M. R.; Ferreira, A. B. B.; Silva, F. A.; Cesarin-Sobrinho, D.; Netto-Ferreira, J. C.; *J. Fluorine Chem.* **2017**, *199*, 30. [Crossref]
43. Berman, H.; Henrick, K.; Nakamura, H.; *Nat. Struct. Mol. Biol.* **2003**, *10*, 980. [Crossref]
44. Hein, K. L.; Kragh-Hansen, U.; Morth, J. P.; Jeppesen, M. D.; Otzen, D.; Moller, J. V.; Nissen, P.; *J. Struct. Biol.* **2010**, *171*, 353. [Crossref]
45. Shao, Y.; Molnar, L. F.; Jung, Y.; Kussmann, J.; Ochsenfeld, C.; Brown, S. T.; Gilbert, A. T. B.; Slipchenko, L. V.; Levchenko, S. V.; O'Neill, D. P.; DiStasio Jr., R. A.; Lochan, R. C.; Wang, T.; Beran, G. J. O.; Besley, N. A.; Herbert, J. M.; Lin, C. Y.; Van Voorhis, T.; Chien, S. H.; Sodt, A.; Steele, R. P.; Rassolov, V. A.; Maslen, P. E.; Korambath, P. P.; Adamson, R. D.; Austin, B.; Baker, J.; Edward F. C. Byrd, E. F. C.; Dachsel, H.; Doerksen, R. J.; Andreas Dreuw, A.; Dunietz, B. D.; Dutoi, A. D.; Furlani, T. R.; Gwaltney, S. R.; Heyden, A.; Hirata, S.; Hsu, C.-P.; Kedziora, G.; Khalliulin, R. Z.; Klunzinger, P.; Lee, A. M.; Lee, M. S.; Liang, W.; Lotan, I.; Nair, N.; Peters, B.; Proynov, E. I.; Pieniazek, P. A.; Rhee, Y. M.; Ritchie, J.; Rosta, E.; Sherrill, C. D.; Simmonett, A. C.; Subotnik, S. E.; Woodcock III, H. L.; Zhang, W.; Bell, A. T.; Chakraborty, A. K.; Chipman, D. M.; Keil, F. J.; Warshel, A.; Hehre, W. J.; Schaefer III, H. F.; Kong, J.; Krylov, A. I.; Gilla, P. M. W.; Martin Head-Gordon, M.; *Phys. Chem. Chem. Phys.* **2006**, *8*, 3172. [Crossref]
46. Hehre, W. J.; *A Guide to Molecular Mechanics and Quantum Chemical Calculations*; Wavefunction, Inc.: Irvine, USA, 2003.
47. Shao, Y.; Molnar, L. F.; Jung, Y.; Kussmann, J.; Ochsenfeld, C.; Brown, S. T.; *Spartan*; Wavefunction, Inc., Irvine, CA, USA, 2003.
48. GOLD 2022.3.0, http://www.ccdc.cam.ac.uk/solutions/csd-discovery/components/gold/, accessed in January 2024.
49. Jones, G.; Willett, P.; Glen, R. C.; Leach A. R.; Taylor, R.; *J. Mol. Biol.* **1997**, *267*, 727. [Crossref]

50. Jones, G.; Willett, P.; Glen, R. C.; Leach A. R.; Taylor, R.; *GOLD*; Cambridge Crystallographic Data Centre, Cambridge, CB2 1EZ, UK, 1997.
51. Protein-Ligand Interaction Profiler, https://plip-tool.biotec.tu-dresden.de/plip-web/plip/index, accessed in January 2024.
52. Adasme, M. F.; Linnemann, K. L.; Bolz, S. N.; Kaiser, F.; Salentin, S.; Haupt, V. J.; Schroeder, M.; *Nucl. Acids Res.* **2021**, *49*, W530. [Crossref]
53. Salentin, S.; Schreiber, S.; Haupt, V. J.; Adasme, M. F.; Schroeder, M.; *Nucleic Acids Res.* **2015**, *43*, W443. [Crossref]
54. Schrodinger, L. L. C.; *PyMOL Molecular Graphics System*, version 2.4.1, DeLano Scientific, San Carlos, CA, USA, 2002.
55. Yuan, S.; Chan, H. C. S.; Hu, Z.; *WIREs Comput. Mol. Sci.* **2017**, *7*, e1298. [Crossref]
56. Rabbani, G.; Baig, M. H.; Jan, A. T.; Lee, E. J.; Khan, M. V.; Zaman, M.; Farouk, A.-E.; Khan, R. H.; Choi, I.; *Int. J. Biol. Macromol*. **2017**, *105*, 1572. [Crossref]
57. Rabbani, G.; Lee, E. J.; Khurshid, A.; Baig, M. H.; Choi, I.; *Mol. Pharm.* **2018**, *15*, 1445. [Crossref]
58. Lakowicz, J. R.; *Principles of Fluorescence Spectroscopy*; Springer: New York, 2006.
59. Rabbani, G.; Baig, M. H.; Lee, E. J.; Cho, W.- K.; Ma, J. Y.; Choi, I.; *Mol. Pharm.* **2017**, *14*, 1656. [Crossref]
60. Mukherjee, S.; Ganorkar, K.; Kumar, A.; Sehra, N.; Ghosh, S. K.; *Bioorg. Chem*. **2019**, *84*, 63. [Crossref]
61. Chaves, O. A.; Iglesias, B. A.; Serpa, C.; *Molecules* **2022**, *27*, 5341. [Crossref]
62. Chaves, O. A.; Jesus, C. S. H.; Cruz, P. F.; Sant'Anna, C. M. R.; Brito, R. M. M.; Serpa, C.; *Spectrochim. Acta, Part A* **2016**, *169*, 175. [Crossref]
63. Montalti, M.; Credi, A.; Prodi, L.; Gandolfi, M. T.; *Handbook of Photochemistry*; CRC Press Taylor & Francis: Boca Raton, 2006.
64. Albani, J. R.; *J. Fluoresc*. **2007**, *17*, 406. [Crossref]
65. Amiri, M.; Jankeje, K.; Albani, J. R.; *J. Fluoresc*. **2010**, *20*, 651. [Crossref]
66. Bolattin, M. B.; Nandibewoor, S. T.; Joshi, S. D.; Dixit, S. R.; Chimatadar, S. A.; *Ind. Eng. Chem. Res.* **2016**, *55*, 5454. [Crossref]
67. Gałęcki, K.; Hunter, K.; Daňková, G.; Rivera, E.; Tung, L. W.; Sherry, K. M.; *J. Lumin.* **2016**, *177*, 235. [Crossref]
68. Moreno, M. J.; Loura, L. M. S.; Martins, J.; Salvador, A.; Velazquez-Campoy, A.; *Int. J. Mol. Sci*. **2022**, *23*, 9757. [Crossref]
69. Naveenraj, S.; Anandan, S.; *J. Photochem. Photobiol.: C* **2013**, *14*, 53. [Crossref]
70. Yang, F.; Zhang, Y.; Liang, H.; *Int. J. Mol. Sci*. **2014**, *15*, 3580. [Crossref]
71. Ross, P. D.; Subramanian, S.; *Biochemistry* **1981**, *20*, 3096. [Crossref]
72. Hirata, K.; Kawai, A.; Chuang, V. T. G.; Sakurama, K.; Nishi, K.; Yamasaki, K.; Otagiri, M.; *ACS Omega* **2022**, *7*, 4413. [Crossref]
73. Lee, P.; Wu, X.; *Curr. Pharm. Des.* **2015**, *21*, 1862. [Crossref]
74. Gao, H.; Lei, L.; Liu, J.; Kong, Q.; Chen, X.; Hu, Z.; *J. Photochem. Photobiol.: A* **2004**, *167*, 213. [Crossref]
75. Chaves, O. A.; Acunha, T. V.; Iglesias, B. A.; Jesus, C. S. H.; Serpa, C.; *J. Mol. Liq.* **2020**, *301*, 112466. [Crossref]
76. Abdullah, S. M. S.; Fatma, S.; Rabbani, G.; Ashraf, J. M.; *J. Mol. Struct.* **2017**, *1127*, 283. [Crossref]
77. Varshney, A.; Rehan, M.; Subbarao, N.; Rabbani, G.; Khan, R. H.; *PLoS One* **2011**, *6*, e17230. [Crossref]

Submitted: October 30, 2023
Published online: March 28, 2024